

Two novel Anderson-type polyoxometalate based Mn^{III} complexes constructed from pyrene derivatives: Synthesis, photophysical, and electrochemical properties

Seda Cetindere^{a,*}, Husniye Ardic Alidagi^a, Montaha Anjass^{b,c}

^a Department of Chemistry, Gebze Technical University, Gebze, Kocaeli, Turkey

^b Institute of Inorganic Chemistry I, Ulm University Albert-Einstein-Allee 11, 89081 Ulm, Germany

^c Helmholtz-Institute Ulm Helmholtzstr. 11, 89081 Ulm, Germany

A B S T R A C T

Keywords:

Pyrene
Polyoxometalate
Anderson
Organic–inorganic hybrid compounds

Symmetrical chloride-functionalized Anderson type POM afterwards used as a building block for onward POM post-functionalization with organic pyrene compounds and two novel organic–inorganic hybrid pyrene-POM compounds were designed, synthesized, and fully characterized. Photophysical and electrochemical properties of these compounds were investigated. Organic–inorganic hybrids retained the unique photophysical properties of their precursor pyrene compounds. Additionally, functionalization of inorganic POM moiety with organic bis-pyrene compound influenced the redox properties of the Mn-Anderson core.

1. Introduction

Polyoxometalates (POMs) are metal oxide clusters that have different structural types and unique properties like, optic, electronic, and magnetic properties, and unique chemical reactivity [1–4]. Therefore, POMs have attracted great attention in recent years for the development of materials and functional devices [5,6]. POMs are ideal precursors for designing and synthesizing new organic–inorganic hybrids with desired functions because of their rich oxygen surface, when they are functionalized by organic, organometallic, and metal–organic groups [7–11]. Because of organic covalently bonded POMs (hybrid compounds) are involving electron-transfer from organic donors to inorganic POMs acceptors, they showed promising applications in functional devices for the photo conversion of light into energy such as photovoltaic cells and artificial photosynthetic devices [12–15]. Since POMs are only photoactive in the UV region, organic dyes play a key role in light-harvesting and transfer the excited electrons to POMs. POMs can be bonded to organic groups covalently, and these hybrid molecules generally show different negative charges, chemically tuneable luminescence activity, and high photo-stability [16]. On the other hand, the design and synthesis of conformationally stable pyrene systems is very interesting because of the strong π - π interactions they create. Electron-enriched pyrene derivatives play a prominent role in improvement of electroluminescent devices due to their easy processing, good thermal

stability, high luminescence efficiency, long fluorescent lifetimes, and tendency to constitute excimers via π - π interactions [17–23].

The development of peripheral binding sites on POMs with organic dyes molecules for the formation of organic–inorganic hybrid systems is significant for wide applications [24–26]. It is clear that organic fragments can dramatically affect the inorganic oxides structures, therefore providing a route for the design of new materials. These organic–inorganic hybrids will combine the advantages of organic molecules like structural fine tuning, and the close interaction and synergistic effects of organic group and inorganic cluster. Since the Anderson cluster forms a planar arrangement of six edge-sharing [MoO₆] units, the resulting {Mo₆} ring is well suited for further ligand binding on either side of the Mo framework. The structural environment of Anderson-type POMs provides direct attachment of an organic fragment to the metal oxide lattice. This strategy allows the development of stable building blocks composed of covalently bonded inorganic POMs and organic species. Moreover, functionalization of the cluster framework can be designed separately by symmetric or non-symmetric closure of the two existing binding sites. In this consideration, we designed and synthesized two novel organic–inorganic hybrid pyrene-Anderson POM compounds (POM1, POM2) as shown in Fig. 1. This study is based on the envisioned post-functionalization method which is a nucleophilic substitution reaction between symmetrical chloride-functionalized POM (POM_{Cl}) and organic pyrene compounds (L1, L2). In these compounds

* Corresponding author at: CETINDERE, Department of Chemistry, Gebze Technical University, P.O.Box: 141, Gebze 41400, Kocaeli, Turkey.
E-mail address: sdemirer@gtu.edu.tr (S. Cetindere).

(POM1, POM2), the inorganic Anderson-type POM based on Mn^{III} (POM_{Cl}) is covalently attached to the luminescent organic pyrene derivatives (L1, L2) over the tris(hydroxymethyl)-aminomethane (Tris) bridges. The hybrid molecular compounds display three negative charges that are balanced by three tetrabutylammonium (TBA) cations. After full characterization of these compounds, photophysical and electrochemical properties were investigated. POM1 and POM2 retained the unique photophysical properties of their precursors L1 and L2, and functionalization of POM_{Cl} with L2 compound influenced the redox properties of the Mn-Anderson core. The relevant results suggest a new way for design of new charge transfer hybrids of organo-functionalized POMs and give an important guide for optical and electrical device applications.

2. Experimental

2.1. Chemicals and Equipment

All chemicals were purchased commercially and used as received unless mentioned. All the chemical reactions were monitored by thin layer chromatography (TLC) with using silica gel plates (Merck, Kieselgel 60, 0.25 mm thickness) with an F254 indicator. Silica gel (Merck, Kieselgel 60, 230–400 mesh) was used for column chromatography. A Thermo Finnigan Flash 1112 Instrument was used to perform elemental analysis. A Perkin Elmer Spectrum 100 Optica was used for FT-IR measurements. A Bruker Daltonics Microflex LT MALDI-TOF mass spectrometer was used for recording the mass spectra. ^1H and ^{13}C NMR spectra of L1 and L2 were taken in CDCl_3 and POM1 and POM2 were taken in $\text{DMSO}-d_6$ solutions on Varian INOVA 500 MHz spectrometer. UV-vis spectra were measured with a UV spectrophotometer named Shimadzu 2101. Fluorescence emission spectra were measured on a Varian Eclipse spectrofluorometer by using 1 cm path length cuvettes at 25 °C. The fluorescence lifetimes were obtained using Horiba-Jobin-Yvon-SPEX Fluorolog 3-2iHR instrument with FluoroHub-B Single Photon Counting Controller at an excitation wavelength of 470 nm. Signal acquisition was performed using a TCSPC module. The electrochemical experiments were acquired using a Pine Research WaveDriver 200 electrochemical workstation.

2.2. Photophysical measurements

UV-vis and fluorescence spectroscopy techniques were used for photophysical measurements. All the measurements were done in MeCN solutions. Fluorescence lifetimes were directly measured and mono-exponentially calculations were used for all compounds.

2.3. Electrochemical Measurements

DC cyclic voltammetry (CV) experiments were performed on a Pine Research WaveDriver 200 electrochemical workstation equipped with a standard three-electrode setup: working electrode: glassy carbon electrode ($d = 3.0$ mm), quasi reference electrode: Ag wire (in a glass frit containing electrolyte solution), counter electrode: Pt wire. All potentials are quoted relative to the ferrocene/ferrocenium internal standard. All experiments were performed in water-free, de-aerated DMF using $n\text{Bu}_4\text{NPF}_6$ (0.1 M) as supporting electrolyte. The solutions were purged with argon (Ar) for at least 15 min to remove O_2 and kept under a slight positive Ar pressure while performing the experiments.

2.4. Synthesis

Starting POM, $(\text{C}_{16}\text{H}_{36}\text{N})_3\text{[MnMo}_6\text{O}_{18}((\text{OCH}_2)_3\text{C}_3\text{H}_3\text{NOCl})_2]$, (abbreviated as POM_{Cl}) was prepared according to the literature procedure [27]. 3,5-di(pyrene-1-yl) phenol (L2) was also prepared according to the literature procedure [28].

2.4.1. Synthesis of 4-(pyrene-1-yl) phenol (L1)

4-Bromophenol (0.47 g, 2.71 mmol), pyrene-1-boronic acid (1 g, 4.06 mmol), tetrabutylammonium bromide (TBAB) (0.017 g, 0.054 mmol) and Na_2CO_3 (2 M, 14 mL) was dissolved in dry toluene/THF (20 mL/5 mL) in 100 mL reaction flask. The mixture was stirred for 20 min under argon atmosphere at room temperature and then $\text{Pd}(\text{PPh}_3)_4$ (0.09 g, 0.08 mmol) was added. The reaction was controlled with TLC and stirred for 2 days under reflux at 80 °C. After the reaction was finished, it was cooled to room temperature. The reaction mixture extracted with dichloromethane/water and organic phase was dried over Na_2SO_4 . Then, the solvent was evaporated under reduced pressure. The residue

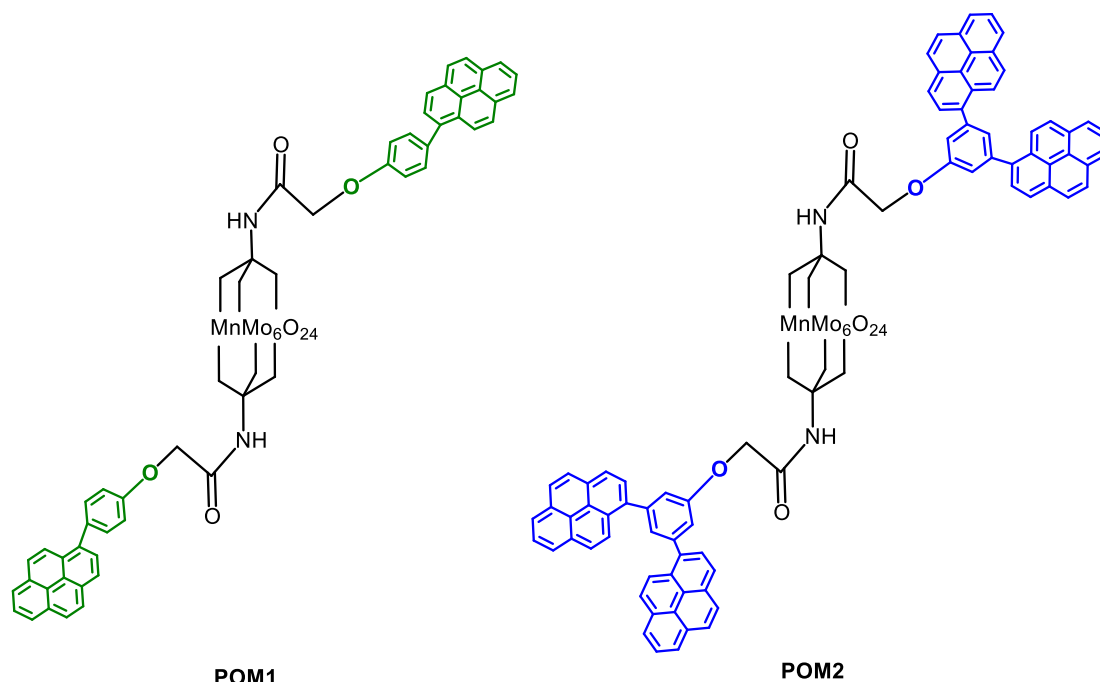


Fig. 1. Molecular structures of POM1 and POM2.

was purified by column chromatography using *n*-hexane: THF (3:1) solvent system and L1 (0.53 g, 65 %) was obtained. Elemental analysis for (C₂₂H₁₄O)₃ in wt.-% (calcd.): C 89.52 (89.77), H 4.87 (4.79). FT-IR (ν , cm⁻¹): 3292 (-OH), 3047 (Ar-CH), 1594 (Ar-C=C), 1169 (Ar-C-O). MS (MALDI-TOF) *m/z* (%): Calc. 294.35, found 295.506 [M + H]⁺. ¹H NMR (in CDCl₃): δ (ppm) 8.22–8.15 (m, 4H, Ar-CH), 8.09 (s, 1H, Ar-CH), 8.04–7.96 (m, 4H, Ar-CH), 7.52 (d, 2H, *J* = 2.1 Hz, Ar-CH), 7.04 (d, 2H, *J* = 6.5 Hz, Ar-CH), 5.15 (s, 1H, -OH).

2.4.2. Synthesis of POM1

POM_{Cl} (0.05 g, 0.025 mmol) was treated with L1 (0.015 g, 0.05 mmol) in dry DMF and stirred under reflux at 80 °C. The progress of the reaction was monitored by taking a sample from the reaction mixture and recovering the POM by precipitation in diethyl ether, after which an IR absorbance spectrum was taken. The disappearance of the -OH peak at 3200 cm⁻¹ assigned to finished reaction. The solvent was removed with rotary evaporator. A minimal amount of fresh MeCN was added to redissolve the POM and the solution was added dropwise to an excess of diethyl ether. The precipitate was collected by centrifugation and subsequently the remaining solid was washed with water, diethyl ether, and dried in air. POM1, (C₁₆H₃₆N)₃-[MnMo₆O₁₈((OCH₂)₃C₃H₃NO-C₂₂H₁₃O)₂], (0.025 g) was obtained in 40 % yield. Elemental analysis for (C₁₆H₃₆N)₃-[MnMo₆O₁₈((OCH₂)₃C₃H₃NOC₂₂H₁₃O)₂] in wt.-% (calcd.): C 48.52 (48.97), H 5.99 (6.01), N 2.70 (2.75). FT-IR (ν , cm⁻¹): 3257 (w), 3089 (w), 2965 (C-H, m), 2926 (C-H, m), 2877 (C-H, m), 1680 (C=O, s), 1558 (m), 1477 (m), 1411 (w), 1365 (w), 1324 (w), 1278 (w), 1186 (w), 1113 (m), 1050 (s), 943 (Mo = O, vs), 918 (Mo = O, vs), 895 (Mo = O, vs), 813 (m), 655 (Mo-O-Mo, vs), 567 (w). MS (MALDI-TOF) *m/z*: Calc. 2550.91, found 1851.27 [M - 3TBA]⁺. ¹H NMR (in DMSO-d₆) δ (ppm): 65.94 (br, 12H, O-CH₂-C), 9.82 (s, 2H, -NH), 8.31–8.13 (m, 8H, Hpy), 8.09 (s, 2H, Hpy), 8.04–7.96 (m, 8H, Hpy), 7.44 (d, 4H, Haro), 7.02 (d, 4H, Haro), 3.61 (s, 4H, CO-CH₂-O), 3.11 (m, 24H, H_{TBA}), 1.52 (m, 24H, H_{TBA}), 1.28 (m, 24H, H_{TBA}), 0.90 (t, 36H, H_{TBA}).

2.4.3. Synthesis of POM2

POM_{Cl} (0.03 g, 0.015 mmol) was treated with L2 (0.015 g, 0.03 mmol) in dry DMF and stirred under reflux at 80 °C. The progress of the reaction was monitored by taking a sample from the reaction mixture and recovering the POM by precipitation in diethyl ether, after which an IR absorbance spectrum was taken. The disappearance of the -OH peak at 3200 cm⁻¹ assigned to finished reaction. The solvent was removed with rotary evaporator under reduced pressure. A minimal amount of fresh MeCN was added to redissolve the POM and the solution was added dropwise to an excess of diethyl ether. The precipitate was collected by centrifugation and subsequently the remaining solid was washed with water, diethyl ether, and then dried in air. POM2, (C₁₆H₃₆N)₃-[MnMo₆O₁₈((OCH₂)₃C₃H₃NOC₃₈H₂₁O)₂], (0.02 g) was obtained in 45 % yield. Elemental analysis for (C₁₆H₃₆N)₃-[MnMo₆O₁₈((OCH₂)₃C₃H₃NOC₃₈H₂₁O)₂] in wt.-% (calcd.): C 54.42 (54.60), H 5.79 (5.83), N 2.38 (2.41). FT-IR (ν , cm⁻¹): 3278 (w), 3054 (w), 2968 (C-H, m), 2929 (C-H, w), 2878 (C-H, m), 1671 (C=O, s), 1571 (m), 1474 (m), 1421 (w), 1369 (w), 1334 (w), 1261 (w), 1108 (m), 1039 (s), 933 (Mo = O, vs), 916 (Mo = O, vs), 863 (Mo = O, vs), 807 (m), 654 (Mo-O-Mo, vs), 563 (w). MS (MALDI-TOF) *m/z*: Calc. 2951.38, found 2175.21 [M - 3TBA]⁺. ¹H NMR (in DMSO-d₆) δ (ppm): 64.09 (br, 12H, O-CH₂-C), 10.13 (s, 2H, -NH), 8.40 (s, 4H, Hpy), 8.39–8.11 (m, 36H, Hpy), 7.26 (s, 2H, Haro), 3.52 (s, 4H, CO-CH₂-O), 3.14 (m, 24H, H_{TBA}), 1.55 (m, 24H, H_{TBA}), 1.29 (m, 24H, H_{TBA}), 0.92 (t, 36H, H_{TBA}).

3. Results and discussion

3.1. Synthesis

We designed and synthesized two new organic-inorganic hybrid compounds based on luminescent pyrene derivatives and Anderson type POM. The attachment of organic moieties onto this inorganic platform

via the tris-ligand esterification method or by post-functionalization has been deeply investigated in the last decade [27,29–32]. In this work, we used the chloro-functionalized Anderson-type POM (POM_{Cl}) and pyrene derivatives (L1 and L2) to obtain symmetrical compounds (POM1 and POM2). In the first step, we prepared the starting compound POM_{Cl} and L2 according to the literature procedures [27,28] and pyrene-derivative (L1). The synthetic route for the ligands L1 and L2 was outlined in Scheme 1. Pyrene derivative (L1) was synthesized utilizing Pd-catalyzed Suzuki cross-coupling reactions of pyrene-1-boronic acid with bromine derivatives in the presence of 2 M Na₂CO₃(aq) as base and TBAB as phase transfer catalyst in THF/toluene solvent mixture in high yields. The synthesized pyrene derivative (L1) has been characterized by ¹H, ¹³C NMR, FT-IR, mass spectrometry and elemental analysis. All the results are consistent with the predicted structures as shown in the experimental section (Fig. 2) and supporting information (SI) (Fig. S1-S3). ¹H NMR spectra of compound L1 was shown in Fig. S2a. The proton signals of aromatic groups on the pyrene ring were observed in the region 8.22–7.96 ppm and benzene ring proton signals at 7.52 and 7.04 ppm, respectively. The proton signal of the -OH on the benzene group which disappeared after D₂O exchange was observed at 5.15 ppm as shown in Fig. S2b. The integration of the aromatic proton signals to the OH group signal in the ¹H NMR spectrum of compound L1 gave approximately a 13:1 proton ratio, which confirmed the suggested structure. In addition, the O-H stretching vibration band at 3292 cm⁻¹ of compounds L1, seen in the FT-IR spectra also support the structure (Fig. 2a).

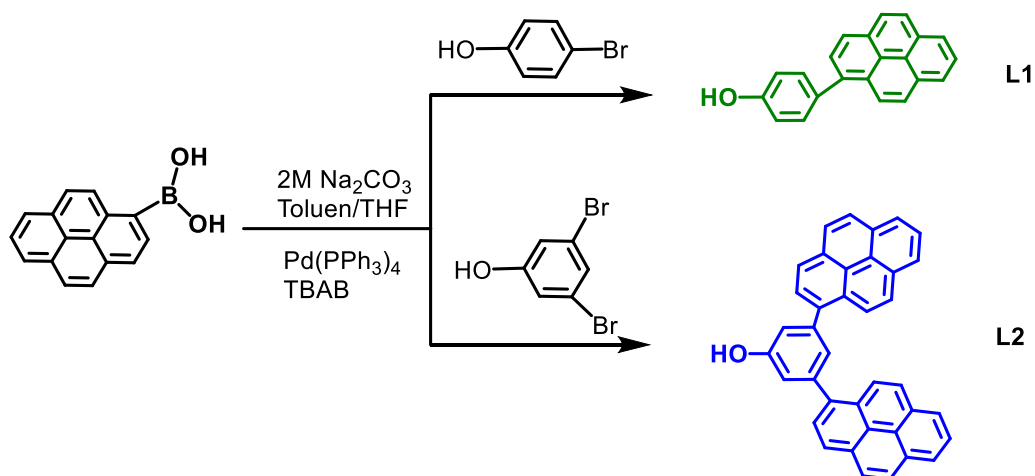
In the second step, we prepared the organic-inorganic hybrid compounds (POM1 and POM2) (Fig. 1). The synthetic route for the compounds (POM1 and POM2) was outlined in Scheme 2. The reactions were followed by FT-IR spectroscopy, where the disappearance of the -OH peak at 3200 cm⁻¹ was a clear indication of the course of the reaction (Fig. 2). These compounds have been fully characterized by FT-IR (Fig. 2), matrix-assisted laser desorption/ionization mass spectrometry (MALDI-MS) (Fig. 3), ¹H NMR spectrometry (Fig. S4-S5), and elemental analysis.

3.2. Photophysical properties

Following the synthetic part, photophysical properties of the compounds (L1, L2, POM1 and POM2) were investigated via UV-vis and fluorescence spectroscopy at room temperature. We have been able to change the physical properties of the POM cluster dramatically, by tethering the highly delocalized aromatic pyrene derivatives covalently to the POM clusters through the tris connector. As shown in Fig. 4a, absorption peak of π - π^* transitions for the compounds are seen at 348 and 280 nm for L1 and POM1 and at 349 and 281 nm for L2 [28] and POM2. As shown in Fig. 4b, the pyrene derivatives (L1 and L2) exhibits emission band at 386 nm upon excitation at 330 nm. Considering that the pyrene derivatives are the luminescence-active center in our hybrid molecules, it was expected that emission peaks for the POM compounds (POM1 and POM2) be also seen at the same nm values as shown in Fig. 4b. Normalized excitation and normalized emission spectra of the compounds were also given in Fig. S6. Fluorescence lifetimes were found to be 8.95 ± 0.009 ns (L1), 14.0 ± 0.013 ns (L2), 8.84 ± 0.013 ns (POM1) and 13.7 ± 0.014 ns (POM2) by direct measurement and mono exponential calculations (Fig. 5). Fluorescence lifetimes of POMs (POM1 and POM2) are lower than their precursor ligands (L1 and L2). The reason is POMs fluorescence intensities are lower than their precursor ligands at the same concentrations because of quencher POM moieties [33].

3.3. Electrochemical properties

Next, we investigated the electrochemical properties of POM_{Cl}, POM1 and POM2 to assess accessible redox transitions in these species. As shown in Fig. 6, cyclic voltammetry of the POM-precursor, POM_{Cl}



Scheme 1. Synthesis pathway of L1 and L2.

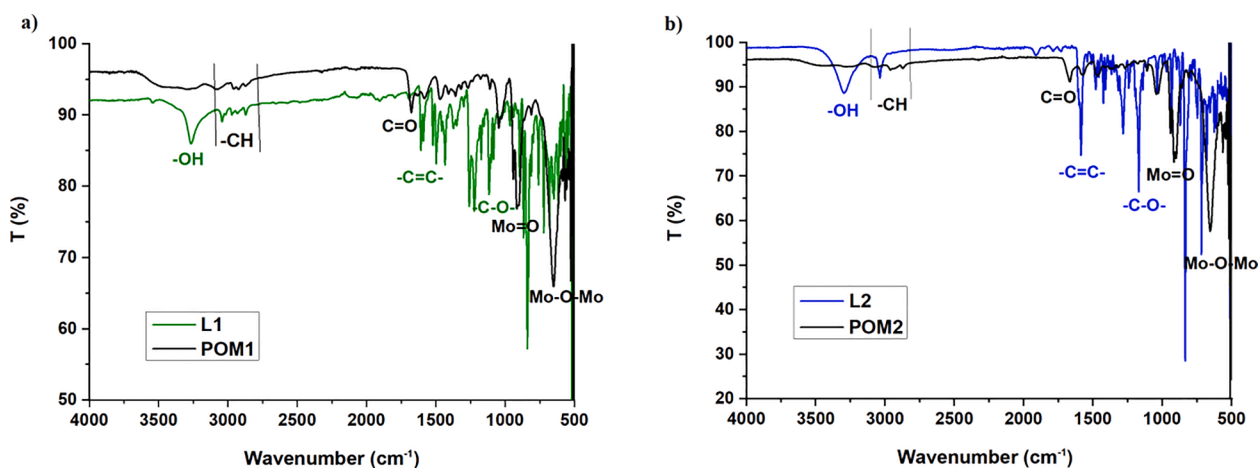
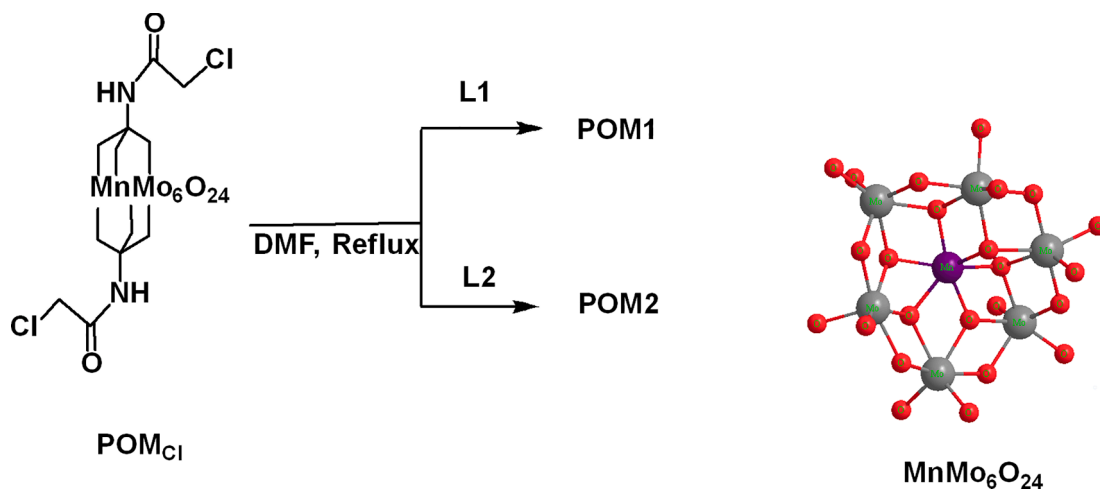


Fig. 2. FT-IR spectra of a) L1 and POM1 and b) L2 and POM2.



Scheme 2. Synthesis pathway of POM1 and POM2.

shows two quasi-reversible redox-transitions, assigned to the $\text{Mn}^{\text{IV/III}}$ couple (I/I', $E_m = 0.32$ V, all potentials given vs Fc^+/Fc), and one $\text{Mn}^{\text{III/II}}$ couple (II/II', $E_m = -1.19$ V), respectively [33,34]. In POM1, the two processes are retained with virtually no potential changes, i.e., $E_m = 0.33$ V (I/I') and $E_m = -1.20$ V (II/II'). In contrast, cyclic voltammogram

of POM2 shows the $\text{Mn}^{\text{IV/III}}$ redox couple (I/I') at $E_m = 0.32$ V, while the $\text{Mn}^{\text{III/II}}$ redox couple (II/II', $E_m = -0.92$ V) is shifted oxidatively from the POM_{Cl} and POM1, indicating that functionalization of POM_{Cl} with L2 influences the redox properties of the Mn-Anderson core. Additionally, POM2 shows irreversible oxidation and reduction peaks (marked with

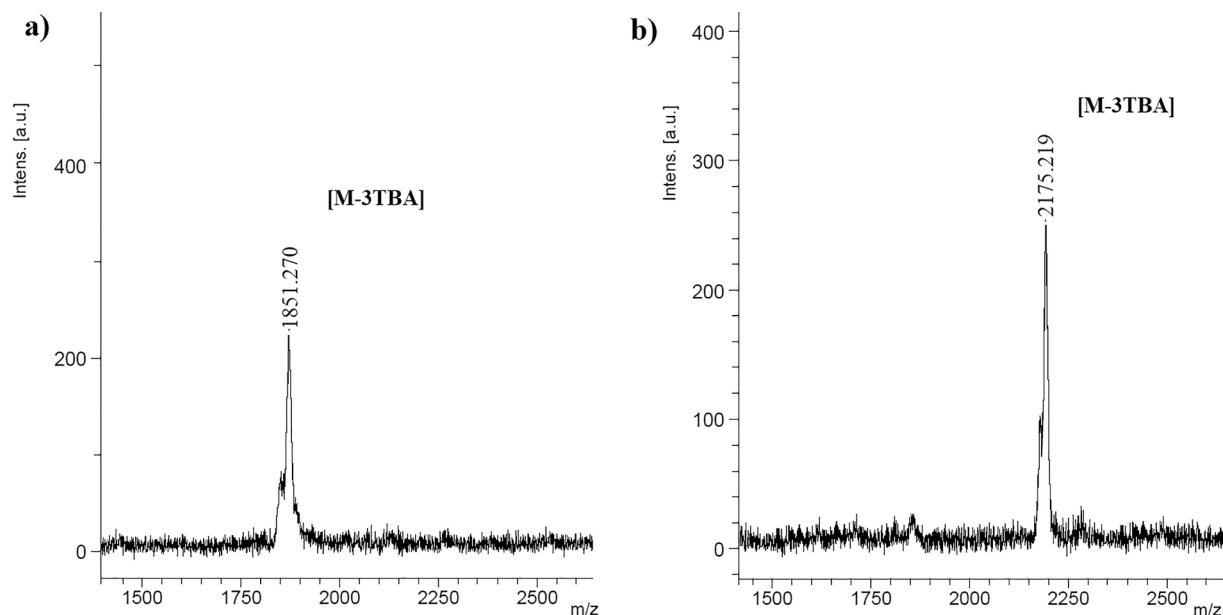


Fig. 3. MALDI-MS spectra of a) POM1 and b) POM2.

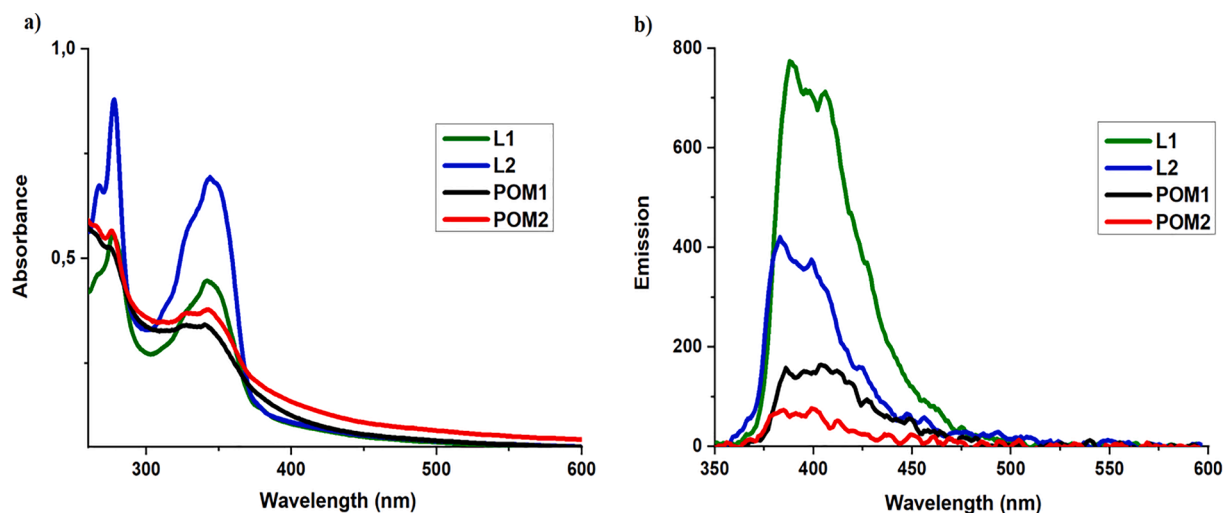


Fig. 4. (a) UV-vis spectra of the compounds (b) Emission spectra of the compounds (10^{-5} M concentrations in MeCN, λ_{exc} = 330 nm).

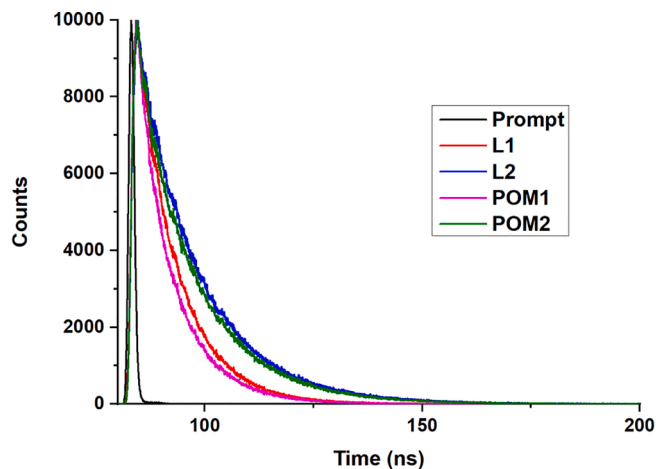


Fig. 5. Fluorescence lifetime spectra of the compounds.

asterisks) at $E = 0.63$ V and $E = -1.44$ V, respectively. These two peaks are assigned to L2, see Fig. S7.

4. Conclusion

In conclusion, two new organic-inorganic hybrids, where pyrene derivatives are covalently bonded to the Anderson type POM clusters were prepared and fully characterized. Here we demonstrated that a nucleophilic substitution reaction can be successfully used as a post-functionalization method for the Anderson-type POM. Photophysical and electrochemical properties of the compounds were investigated and compared with their precursor POM and pyrene moieties. The results clearly demonstrate that the attachment of organic pyrene compounds to the Anderson-type core gained fluorescence properties to the inert POM cluster. Also, functionalization of inorganic POM moiety with organic bis-pyrene compound influenced the redox properties of the Anderson POM core. Furthermore, we believe that these results might offer a new way for the design of new organic-inorganic hybrid pyrene-POM compounds for optical and electrical device applications. Further

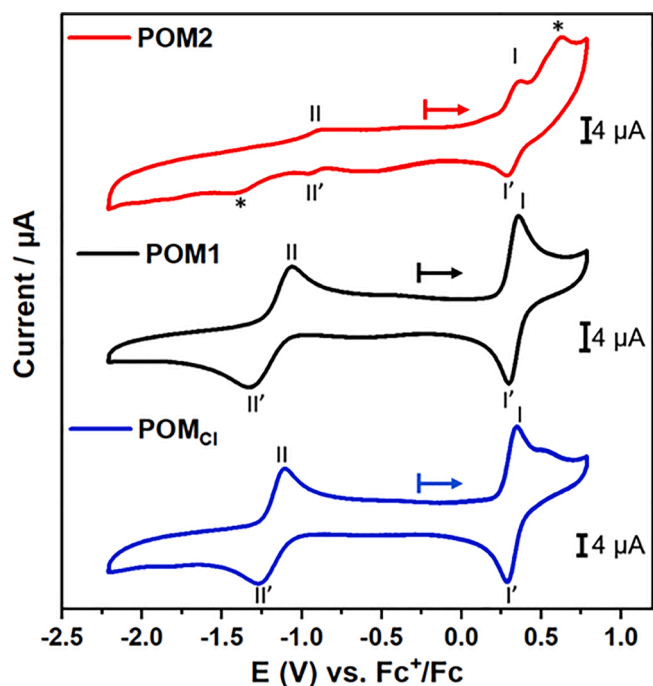


Fig. 6. Cyclic voltammetry of POM_{Cl}, POM1 and POM2. Conditions: water-free, de-aerated DMF containing 0.1 M (nBu₄N) PF₆, scan rate: 0.1 V s⁻¹, [analyte]: 1 mM.

studies on this topic continue in our laboratories.

Declaration of Competing Interest

The authors declare that they have no known competing financial interests or personal relationships that could have appeared to influence the work reported in this paper.

Data availability

The data that has been used is confidential.

References

- [1] A. Proust, R. Thouvenot, P. Gouzerh, *Chem. Commun.* (2008) 1837–1852.
- [2] Z.H. Peng, *Angew. Chem. Int. Ed.* 43 (2004) 930–935.
- [3] D.L. Long, E. Burkholder, L. Cronin, *Chem. Soc. Rev.* 36 (2007) 105–121.
- [4] M. Yang, Z. Jin, C. Wang, X. Cao, X. Wang, H. Ma, H. Pang, L. Tan, G. Yang, *ACS Appl. Mater. Interfaces* 13 (2021) 55040–55050.
- [5] M. Clemente-Leon, E. Coronado, C.L. Gomez-Garcia, C. Mingotaud, S. Ravaine, G. Romualdo-Torres, P. Delhaes, *Chem.-Eur. J.* 11 (2005) 3979–3987.
- [6] A. Muller, F. Peters, M.T. Pope, D. Gatteschi, *Chem. Rev.* 98 (1998) 239–271.
- [7] J. Geng, M. Li, J.S. Ren, E.B. Wang, X.G. Qu, *Angew. Chem. Int. Ed.* 50 (2011) 4184–4188.
- [8] J. Zhang, J. Hao, Y. Wei, F. Xiao, P. Yin, L. Wang, *J. Am. Chem. Soc.*, 132:1 (2010) 14–15.
- [9] D.L. Long, R. Tsunashima, L. Cronin, *Angew. Chem. Int. Ed.* 49 (2010) 1736–1758.
- [10] C. Allain, D. Schaming, N. Karakostas, M. Erard, J.P. Gisselbrecht, S. Sorgues, I. Lampre, L. Ruhlmann, B. Hasenknopf, *Dalton T* 42 (2013) 2745–2754.
- [11] X. Wang, Z. Feng, B. Xiao, J. Zhao, H. Ma, Y. Tian, H. Pang, L.J.G.C. Tan, *Green Chem.* 22 (2020) 6157–6169.
- [12] Q.S. Yin, J.M. Tan, C. Besson, Y.V. Geletii, D.G. Musaev, A.E. Kuznetsov, Z. Luo, K. I. Hardcastle, C.L. Hill, *Science* 328 (2010) 342–345.
- [13] J. Etedgui, Y. Diskin-Posner, L. Weiner, R. Neumann, *J. Am. Chem. Soc.* 133 (2011) 188–190.
- [14] F. Odobel, M. Severac, Y. Pellegrin, E. Blart, C. Fosse, C. Cannizzo, C.R. Mayer, K. J. Elliott, A. Harriman, *Chem.-Eur. J.* 15 (2009) 3130–3138.
- [15] T. He, J.L. He, M. Lu, B. Chen, H. Pang, W.F. Reus, W.M. Nolte, D.P. Nackashi, P. D. Franzon, J.M. Tour, *J. Am. Chem. Soc.* 128 (2006) 14537–14541.
- [16] C.L. Hill, *Chem. Rev.* 98 (1998) 1–2.
- [17] T.M. Figueira-Duarte, K. Mullen, *Chem. Rev.* 111 (2011) 7260–7314.
- [18] J.C. Xiao, H.M. Doung, Y. Liu, W.X. Shi, L. Ji, G. Li, S.Z. Li, X.W. Liu, J. Ma, F. Wudl, Q.C. Zhang, *Angew. Chem. Int. Ed.* 51 (2012) 6094–6098.
- [19] J.C. Xiao, Y. Divayana, Q.C. Zhang, H.M. Doung, H. Zhang, F. Boey, X.W. Sun, F. Wudl, *J. Mater. Chem.* 20 (2010) 8167–8170.
- [20] J.C. Xiao, S.W. Liu, Y. Liu, L. Ji, X.W. Liu, H. Zhang, X.W. Sun, Q.C. Zhang, *Chemistry-an Asian Journal* 7 (2012) 561–564.
- [21] J.C. Xiao, C.D. Malliakas, Y. Liu, F. Zhou, G. Li, H.B. Su, M.G. Kanatzidis, F. Wudl, Q.C. Zhang, *Chemistry-an Asian Journal* 7 (2012) 672–675.
- [22] Q.C. Zhang, Y. Divayana, J.C. Xiao, Z.J. Wang, E.R.T. Tiekink, H.M. Doung, H. Zhang, F. Boey, X.W. Sun, F. Wudl, *Chem.-Eur. J.* 16 (2010) 7422–7426.
- [23] A.G. Crawford, A.D. Dwyer, Z.Q. Liu, A. Steffen, A. Beeby, L.O. Palsson, D.J. Tozer, T.B. Marder, *J. Am. Chem. Soc.* 133 (2011) 13349–13362.
- [24] X. Wang, J.F. Lin, H. Li, C.Y. Wang, X.L. Wang, *RSC Adv.* 12 (2022) 4437–4445.
- [25] Y.F. Song, D.L. Long, L. Cronin, *Angew. Chem. Int. Ed.* 46 (2007) 3900–3904.
- [26] L. Huang, J. Hu, Y. Ji, C. Streb, Y.-F. Song, *Chem.-Eur. J.* 21 (2015) 18799–18804.
- [27] S. Vanhaecht, J. Jacobs, L. Van Meervelt, T.N. Parac-Vogt, *Dalton T* 44 (2015) 19059–19062.
- [28] H.A. Alidagi, S.O. Tumay, A. Senocak, O.F. Ciftbudak, B. Cosut, S. Yesilot, *New J. Chem.* 43 (2019) 16738–16747.
- [29] D. Mercier, M. Ben Haddada, M. Huebner, D. Knopp, R. Niessner, M. Salmain, A. Proust, S. Boujday, *Sensors and Actuators B-Chemical* 209 (2015) 770–774.
- [30] D. Ma, L.Y. Liang, W. Chen, H.M. Liu, Y.F. Song, *Adv. Funct. Mater.* 23 (2013) 6100–6105.
- [31] J.K. Gao, X.F. Liu, Y. Liu, L.L. Yu, Y.H. Feng, H.Y. Chen, Y.X. Li, G. Rakesh, C.H. A. Huan, T.C. Sum, Y. Zhao, Q.C. Zhang, *Dalton T* 41 (2012) 12185–12191.
- [32] W. Ju, X.L. Song, G. Yan, K. Xu, J. Wang, D.H. Yin, L. Li, X.F. Qu, Y.G. Li, J. Li, *J. Mater. Chem. B* 4 (2016) 4287–4294.
- [33] S. Cetindere, S.T. Clausing, M. Anjass, Y.S. Luo, S. Kupfer, B. Dietzek, C. Streb, *Chem.-Eur. J.* 27 (2021) 17181–17187.
- [34] S. Schonweiz, M. Heiland, M. Anjass, T. Jacob, S. Rau, C. Streb, *Chem.-Eur. J.* 23 (2017) 15370–15376.